

CONNECTING SUBTIDAL AND SUBAERIAL SAND TRANSPORT PATHWAYS IN THE TEXEL INLET SYSTEM

Kathelijne Wijnberg¹, Ad van der Spek², Filipe Galiforni Silva¹, Edwin Elias³,
Mick van der Wegen^{4,2}, and Jill Slingers

Abstract

Potential transport pathways between the subtidal and subaerial part of tidal inlet systems are explored by means of a case study of Texel Inlet, The Netherlands. Based on a morphologic analysis of multi-annual, high-resolution bathymetric and topographic data sets we hypothesize that two mechanisms connect the subtidal and subaerial parts of the system. The first mechanism relates to deposition on the tip of the island occurring to a large extent below spring high tide level, providing a fresh sediment source available for aeolian transport during parts of the tidal cycle. The second mechanism relates to sand deposition on the wide sandflat above spring high tide level occurring during storm surge flooding. These deposits are then available for aeolian transport during regular water levels. Due to the dominant wind direction at Texel Island, this leads to extensive dune formation on the downwind end of the sandflat.

Key words: morphodynamics, tidal inlet, coastal dunes, sandflat, sediment transport pathways

1. Introduction

Tidal inlets are cross-roads for sediment exchange, not only between the open coast and the connected tidal basin but also between the submerged ebb-delta and emerging sand shoals that, once attached to the shore, may induce vertical build-up of the coast above storm surge levels through dune formation. Identifying and understanding the transport pathways of sediment from the subtidal domain onto the barrier island is highly relevant, as the elevation of a barrier island above storm surge water levels is one of the primary factors in barrier island geomorphologic response to storms (e.g. Sallenger, 2000; Rosati and Stone, 2009).

So far, studies on transport pathways from the nearshore to the dunes focused on beach-dune systems away from tidal inlets (e.g. Aagaard et al, 2004; Matias et al. 2009; Anthony, 2013). Dune systems close to inlets, so at the tips of barrier islands, are rarely studied, even though those areas can have wide sandflats and thus an ample source of sand for aeolian transport as well as accommodation space for dunes to grow.

The aim of this paper is to present the first results of connecting the subtidal and subaerial transport pathways in a case study of the Texel Inlet system (Marsdiep), the Netherlands, based on a morphologic analysis of multi-annual, high-resolution bathymetric and topographic data sets.

2. Study area: the Texel Inlet system

The Texel Inlet system is the westernmost inlet connecting the Wadden Sea tidal basin to the North Sea (Figure 1). On the south side, the Texel inlet is bounded by the mainland coast which is protected by a sea dike and groins. To the North, the central inlet channel (Marsdiep) is bordered by a wide sandflat named De Hors (Figure 1a). Texel Inlet is a mixed-energy inlet system. The asymmetric shape of the ebb delta of Texel

¹ Water Engineering&Management, Faculty of Engineering Technology, University of Twente, PO Box 2217, 7500 AE Enschede, The Netherlands. k.m.wijnberg@utwente.nl; f.galifornisilva@utwente.nl

² Deltares, P.O Box 177, 2600 MH, Delft, The Netherlands. ad.vanderspek@deltares.nl

³ Deltares USA Inc, 8070 Georgia Ave, Silver Spring, MD 20910, USA. Edwin.Elias@Deltares-usa.us

⁴ Unesco-IHE, PO Box 3015,2601 DA Delft, The Netherlands. m.vanderwegen@unesco-ihe.org

⁵ Faculty of Technology, Policy and Management, Delft University of Technology, PO Box 5015, 2600 GA, Delft, The Netherlands. j.h.slinger@tudelft.nl

inlet is ascribed to the redistribution of sediments in response to the changed hydrodynamic conditions in and near the inlet following the closure of the Zuiderzee basin in 1932 (Figure 1c). The reduction in the size of the tidal basin by about 5.900 km², induced a phase shift in the inlet tide, resulting in a relocation of the main channels ending up in a configuration with distinctively southward oriented main ebb-channels (1932-1975), that have remained remarkably stable in position ever since (Elias and Van der Spek, 2006) (Figure 1b). However, during this period of overall stabilized geometry major changes have occurred in the northern part of the ebb-delta and the adjacent beach-dune system (see Section 4).

The mean tidal range in the inlet is 1.34 m, with a mean high tide level of +0.65 m NAP, and a mean spring high tide level (MSHTL) of +0.84m NAP. NAP is the Dutch vertical ordnance datum, which is approximately equal to mean sea level (MSL). During the study period of subaerial developments (1997-2015), storm surge levels reached a maximum elevation of +2.71m NAP, flooding the sandflat De Hors all the way to the dunes, which start at an elevation around +2m NAP. Over this studied period, storm surge levels exceeded the 2m level 25 times, but during 8 out of the 18 years storm surge levels did not reach +2m NAP.

Prevailing winds come from southwesterly directions.

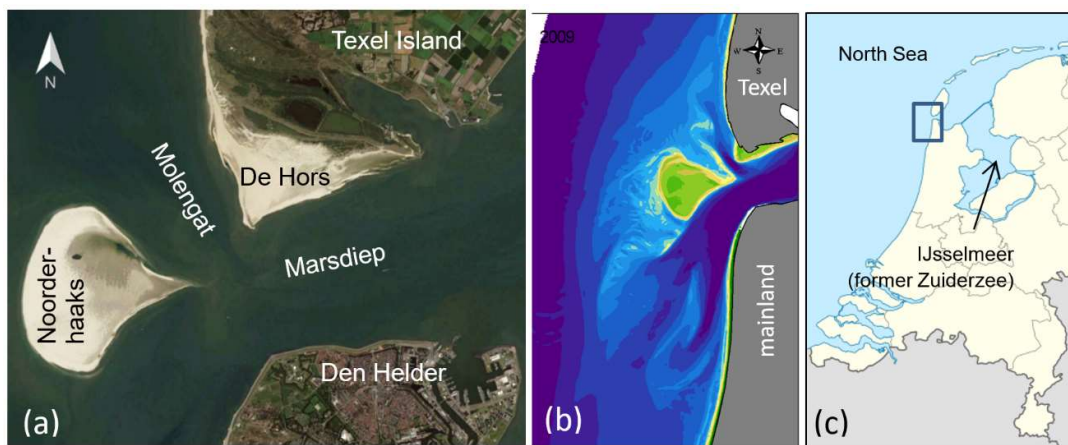


Figure 1. The Texel inlet system (the Netherlands).

3. Materials and methods

The analysis of bathymetric changes and construction of a detailed sediment budget are based on a series of bathymetric datasets, starting from 1986 that are digitally available from the Donar database at Rijkswaterstaat. The maps are based on data collected frequently, in approximately 3-year intervals for the ebb-tidal delta and 6-year intervals for the basin. Following quality checking for measurement errors, data are combined with nearshore coastline measurements, interpolated to a 20x20 m grids and stored digitally as 10x12.5 km blocks called *Vaklodingen*. Each of these maps was visually inspected and clear data outliers or missing (individual) data points were corrected. Maps with missing data along the island shores have been completed using JarKus survey data ('JarKus' is acronym for 'Jaarlijkse Kustmetingen' = Annual Coastal Surveys) or linear interpolation between the nearest available data points. An example of these Digital Elevation Models (DEMs) based on these measurements is presented in Fig. 4.

It must be noted that changes in survey techniques and instruments, positioning systems, and variations in correction and registration methods over time make it difficult to estimate the exact accuracy of the measurements and therefore the DEMs.) The vertical accuracy of *Vaklodingen* data is estimated to range between 0.11 - 0.40 m.

For the analysis of the subaerial morphological evolution, annual LIDAR surveys were used which were obtained from the *Rijkswaterstaat* data base. Topographic data of De Hors sandflat and dunes, were available for the period 1997 to 2015. The vertical accuracy of the data is within 8 cm. Unfortunately, surveys were lacking for the years 2000 and 2002. From 1997 to 2012 data are available on a 5x5 m grid. Later surveys were available at a 2x2m grid, but for consistency in the elevation change computations these were resampled

to a 5x5m grid. Surveys were done around low tide, such that elevation data above -0.3 m NAP are generally available in these surveys.

To characterize the areal changes in the shape of De Hors sandflat contour line maps were visually analyzed. We used contour lines for MSL, mean spring high tide level (MSHTL) and the +1m contour. The MSL contours seemed to act as the most direct indicator of the shoreline erosion related to channel migration. The MSHTL contour outlines the surface area that is generally available for aeolian transport except for storm surge conditions. The +1m contour most clearly outlined interesting ridge development on the southeast facing boundary of De Hors sandflat.

To study patterns in deposition and erosion across De Hors and in the dune area, annual difference maps were created between subsequent surveys (because of the two missing years, two difference maps covered a 2 year interval). Based on the phases of sandflat development extracted from the contour analysis, also difference plot over larger time intervals were created to characterize the erosion–deposition patterns for these phases of sandflat development.

Finally, annual volume changes were calculated for the dune area (elevation changes of at least 0.1m occurring above +2 m NAP), for the accretionary part of the sandflat (elevation increase of at least 0.1 m occurring above MSHTL but below +2m NAP), and for the erosive part of the sandflat (elevation decrease of at least 0.1 m, occurring above MSHTL but below +2m NAP). The 0.1 m threshold was chosen to account for measurement inaccuracy.

Also, a data set of observed highest daily water level was available for the full study period. This data set was created from hourly water level data measured at a tide gauge located in Den Helder harbor, directly opposite to De Hors area (Figure 1a).

4. Co-evolving subtidal and subaerial morphology

4.1. Subtidal morphological evolution

The present-day sediment dynamics in the ebb-tidal delta off Texel inlet (1986-2012) are governed by sediment redistribution on the ebb-tidal delta itself, and by sediment transfer from the ebb-tidal delta to the down-drift island and into the basin. The largest erosion prevails on the western, seaward margin of Noorderhaaks (Figure 2a) where tides and waves are reworking the ebb-shield and transporting the sand landward. Locally, sedimentation and erosion patterns are governed by channel-shoal interaction. On the northern part of the ebb-tidal delta, a distinct spit-like feature called Noorderlijke Uitlopers van de Noorderhaaks (NUN) developed towards the north (Figure 2a). The flood-dominated Molengat channel, located between the northward spit and the coast, is forced to the east (Figure 2c-e) which has induced large sediment losses from the adjacent Texel coastline.

While the seaward side of Noorderhaaks shows large changes, the landward part (Onrust) remained remarkably stable in position over the period 1991-2003. Here, the large flow velocities through Molengat effectively redistributed the landward sediment transports from Noorderhaaks to the north and south. These transports prohibited the NUN to rapidly migrate landward due to the onshore wave-driven transports. The stability of the shoal and spit indicates that near the inlet a balance between along-channel, tide-dominated transports and landward wave-driven transports existed. This stability was clearly present till 2003, but large changes in the eastern tip of Noorderhaaks and adjacent Molengat channel have occurred since. Between Noorderhaaks and Molengat a new flood channel emerged (Figure 2a) that pushed the tip of Noorderhaaks to the south. As a result, the width of the channel between Noorderhaaks and De Hors increased, a clear shift from the deepening and landward migrating trend observed since the 1950's (Figure 2b-d).

This distorted state has large implications for the nearshore and beach of the island of Texel. Prior to 2006, the channel was deep and narrow, with steep embankments (Figure 2b-d). Since 2006 the channel reduces in depth, and the steep channel slopes cannot be maintained. As a result, locally, strong coastal (shoreline) erosion is observed as the channel reduces in slope; the upper part of the profile extends landward due to ongoing wave-driven erosion. By this time the northern tip of the spit has (nearly) merged with the coastline (Fig. 2a; 2006, 2012).

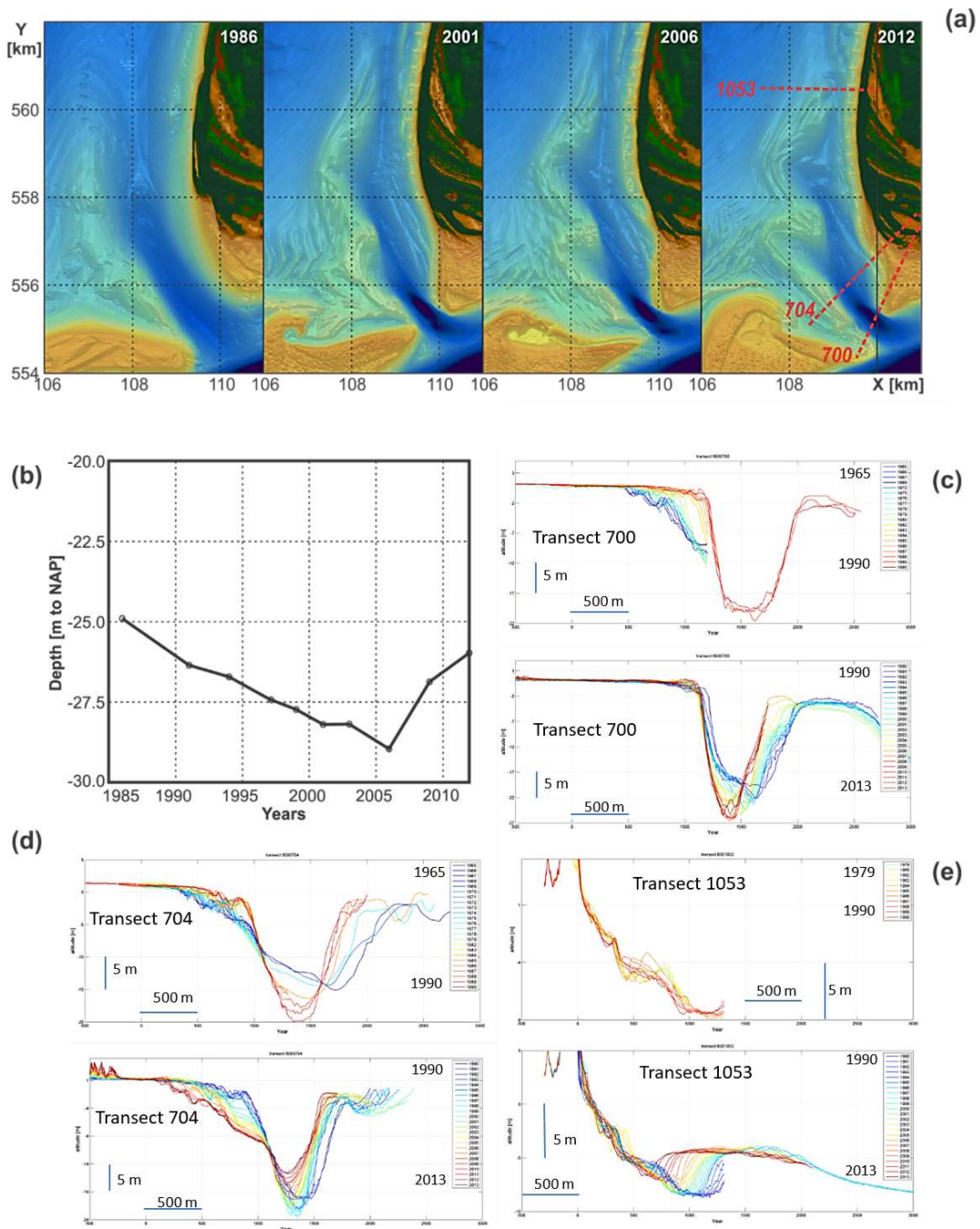


Figure 2. (a) Morphodynamic changes on the northern part of the ebb-tidal delta, including the Noorderlijke Uitlopers van de Noorderhaaks, Molengat channel and De Hors based on Vaklodingen for 1986, 2001, 2006 and 2012. (b). Development of the maximum depth in the Molengat channel, and (c,d,e) Jarkus profiles for transects 700, 704 and 1053 respectively for time frames 1965-1990 (top) and 1990-2013 (bottom). The developments along transect 700 illustrate the relationship between the channel and the sandflat De Hors.

4.2. Subaerial morphological evolution

Plan shape

Figure 3 shows the overall development of the subaerial part of the Texel inlet system over the period 1997-2015. On the north side of the sandflat, the dune system expanded about 0.5km southward, almost doubling in areal extent of the dune system from about 0.78 km² to 1.52 km². On the western and eastern part of the dune area, dune growth occurred mostly by forming a new continuous dune ridge, while in the central part a hummocky dune field developed with 2 to 3 m high dunes. Also a rather isolated big dune developed on the central east part of the sandflat (near $x \approx 2500\text{m}$). The net elevation change of the sandflat was small in comparison to the dune area. Some small deposition occurred on the central part of the sandflat

The sandflat changed in overall plan shape due to the subtidal morphological developments. As visualized in Figure 4, three phases can be distinguished in the development of De Hors sandflat. The first phase (1997-2006) is characterized by a trend of progradation occurring on the central southeast side of the sandflat (I). In the second phase (2007-2011), the shoreline recession trend related to the Molengat channel erosion becomes visible on the central west side of De Hors (II). Note that in 2011 the shoreline starts to prograde already westwards again on the northwestern part of De Hors, after which in the third phase (2012-2015) this shoreline accretion continues (IIIa), showing southward propagating trend as well. At the same time a rapid eastward migration of the southwestern part of De Hors occurs (IIIb).

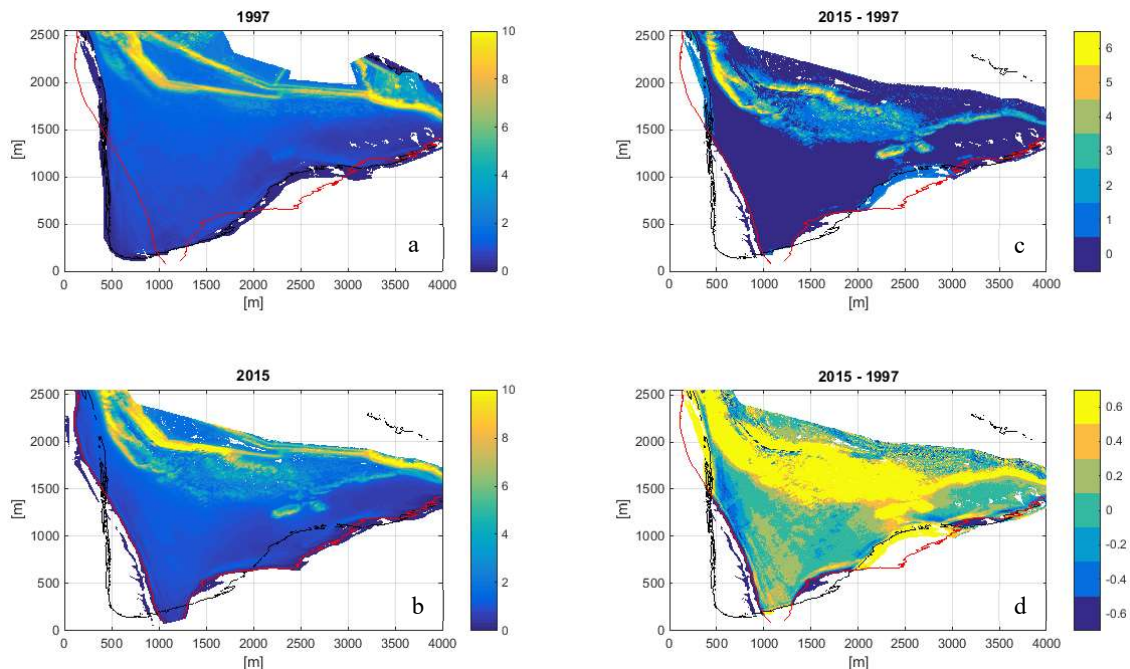


Figure 3. Morphologic change of De Hors sandflat and dune area over the period 1997 to 2015. (a) elevation (m to NAP) in 1997, (b) elevation (m to NAP) in 2015, (c, d) change in elevation between 1997 and 2015 with two differently scaled color bars to emphasize respectively changes in the dune area (top right) and changes on the sandflat (bottom right). In all plots the MSL contour positions in 1997 (black) and 2015 (red) are shown.

Elevation

From the annual elevation change maps, three characteristic erosion/deposition patterns could be observed on the west side of De Hors sandflat (Figure 5). In 11 out of the 14 annual elevation change maps, a shore parallel zone of deposition was observed above MSHTL along the western border of De Hors (Figure 5, b and c). For 4 of those cases, this shore parallel zone of deposition was accompanied by a clear shore parallel zone of erosion seaward of it, also located above MSHTL (Figure 5 b). In the other 3 cases no measurable deposition occurred (less than 0.1 m elevation change) or some small erosion (Figure 5 a). The latter 3 cases

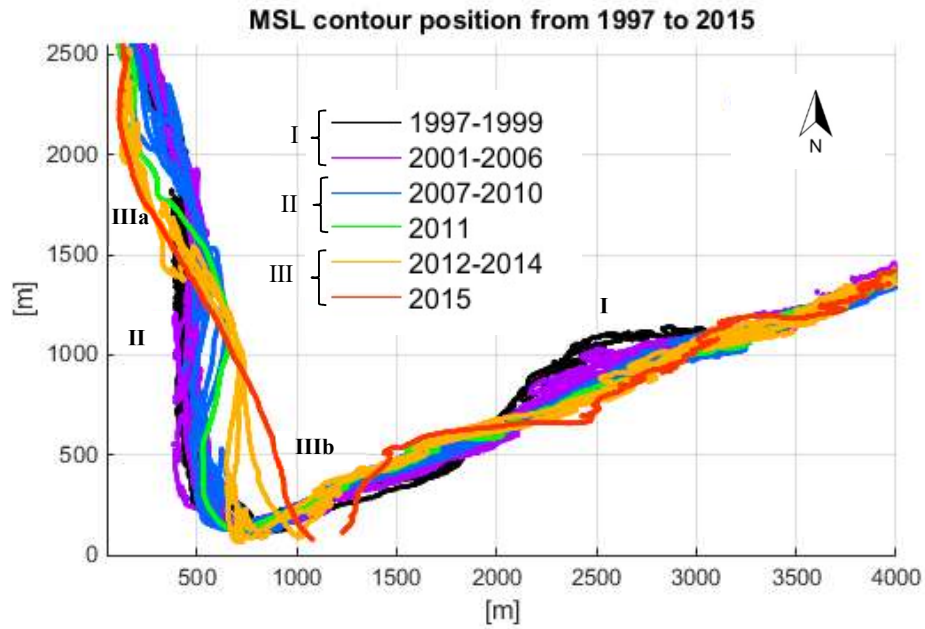


Figure 4. Development of the outline of De Hors sandflat from 1997 to 2015 at a level (MSL) that is affected by hydrodynamic processes on a daily basis. Roman numerals indicate area of interest for respective development phase.

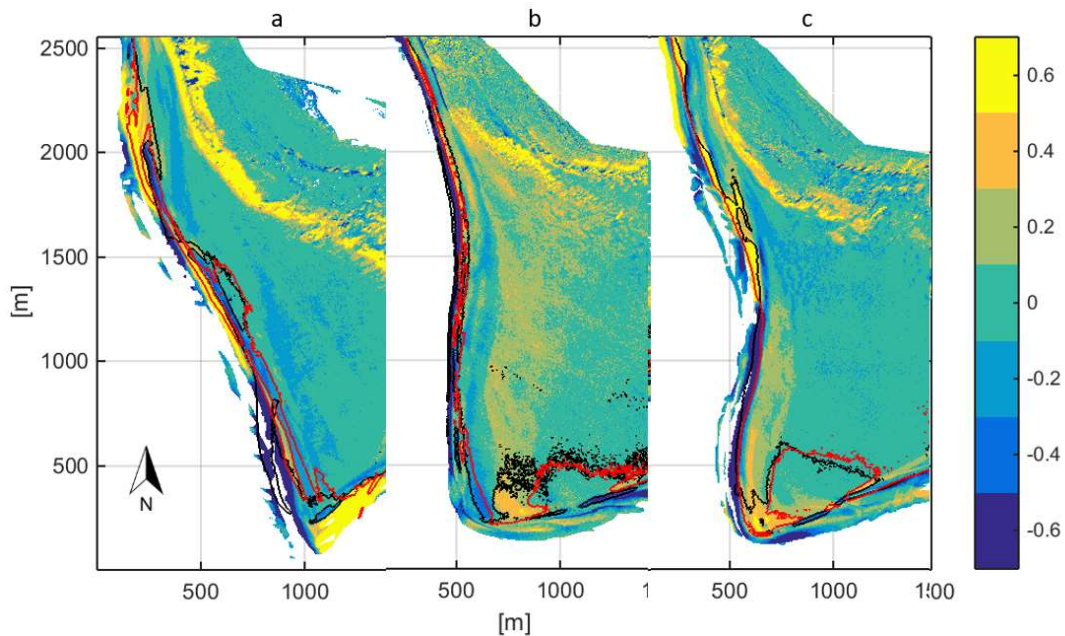


Figure 5. Examples of the three types of sandflat elevation change observed on the west side of the sandflat (see text). In each plot, the position of MSHTL contours are shown for the first year (black) and second year (red). From left to right: elevation change over 2014-2015 (a), 2003-2004 (b), and 2009-2010 (c). Positive values indicate deposition (in m).

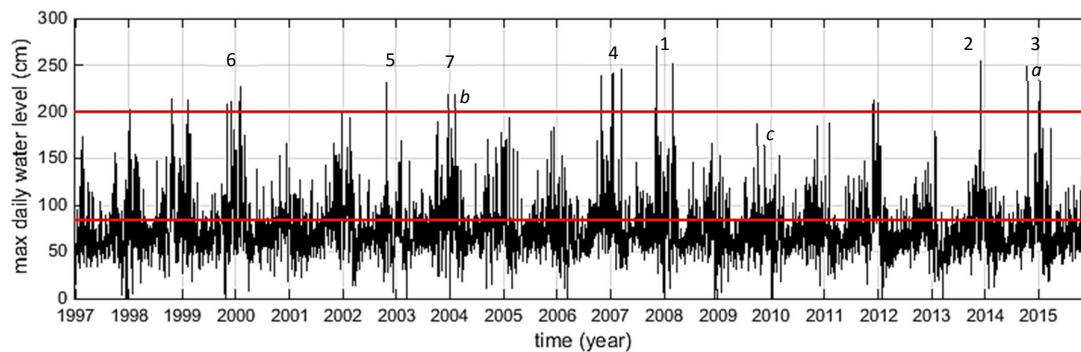


Figure 6. Daily maximum water levels, measured at Den Helder. Lower red line indicates mean spring high tide level (MSHTL) and the upper red line (+2m) indicates approximate elevation above which dune development is present. Numbers indicate ranking of highest observed water level between elevation surveys. Letters indicate the periods for which erosion/deposition patterns are shown in Figure 5.

coincided with the top 3 ranked years with respect to the highest annual storm surge water level between elevation surveys. The 4 cases where parallel zones of erosion and deposition occurred happened to be the years that ranked 4 to 7 with respect to highest annual storm surge levels (Figure 6).

The net elevation changes occurring for the three phases in plan shape development, are shown in Figure 7. The top and middle panel show that the shoreline erosion by the Molengat channel is accompanied by deposition on the western side of the sandflat above MSHTL, as well as deposition near the southern tip of De Hors (also visible in Figure 2c). In the third phase, only minor net deposition above MSHTL occurred on the southwestern part of the sandflat (Figure c), but intertidal deposition near the tip did occur.

Further, along the southeastern border of De Hors, a narrow zone of deposition occurred along the margins of the Marsdiep channel. This zone is highlighted in Figure 7d-g showing the +1m contour position over time in the three phases. Further, it appears from those figures, that in phase III the recovery of the eroded shoreline on the northwestern part of the sandflat is occurring through development of a ridge feature, leaving a depression in the terrain landward of it (Figure 7c and 7g). This resembles a spit like feature indicating southward directed longshore transport.

Volume

Over the 18 year period from 1997 to 2015, the dune area accumulated $2.50 \cdot 10^6$ m³ of sand (Table 1), and accreted almost everywhere. Only at a few locations in the dune system net erosion occurred (Figure 3d). This erosion related to sediment redistribution in the dune system itself, amounting to $-0.05 \cdot 10^6$ m³. The sandflat showed a net gain of sediment over the 18 year period as well, albeit a much smaller amount of only $0.17 \cdot 10^6$ m³. The total erosion volume on the sandflat was an order of magnitude smaller than the total volume of deposition (Table 1).

For each of the three phases of development of the sandflat identified earlier (Figure 3), the sandflat showed a net gain of sediment as well, ranging from $0.21 \cdot 10^6$ m³ in the first phase to $0.03 \cdot 10^6$ m³ in the third phase. The fact that the numbers don't add up to the net volume increase over the full period can be explained by the fact that only volume changes can be calculated for the overlapping areas. These areas are larger for each of the three sub-periods than for the full 18 year period (compare Figure 3d to Figure 7 a-c). Generally erosion volumes on the sandflat are considerably smaller than the deposition volumes, except for the third phase where the deposition volume is relatively small (Table 1). This is the phase in which the tip of the sandflats migrates rapidly eastward. The dune area accretes in each of the three phase as well, with deposition volumes being much larger than the erosion volume. In this case the summation of the net volume increase for the three phase is smaller than the net volume increase over the full 18 year period, because of the way the 2 m criterion is applied. Due to a consistently expanding dune area, this resulted in a 'deeper' aeolian deposition zone for the full 18 year period, than for each of the sub-periods.

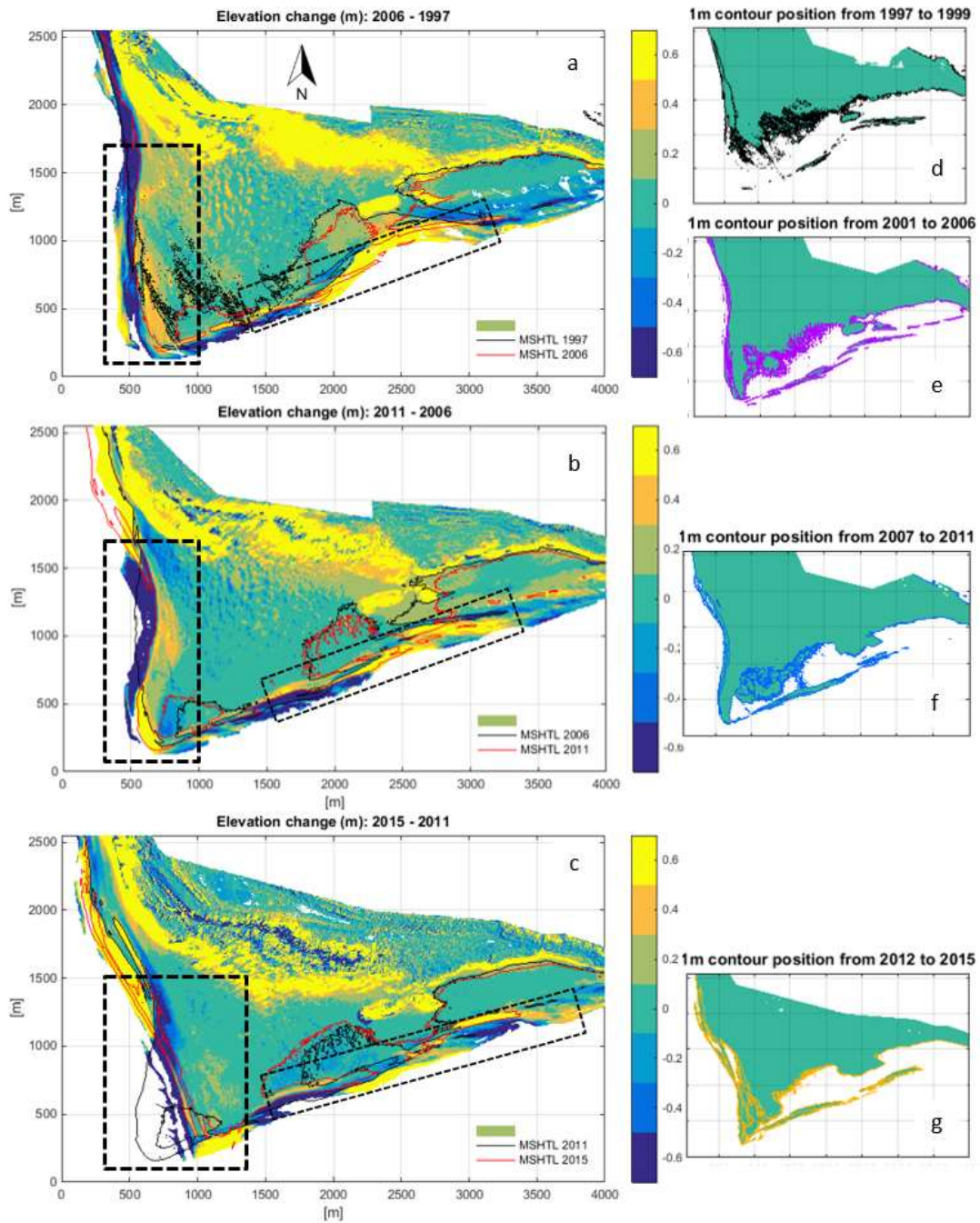


Figure 7. Topographic changes in De Hors area. Left-hand panels (a-c): elevation change on De Hors for the three main phases of sandflat development. Right-hand panels (d-g): position +1m contour highlighting topographic changes along the edges of De Hors sandflat above MSHTL

Table 1. Volume changes of De Hors sandflat and dune area over various time intervals.

Period	Total volume change (10^6 m^3)					
	Dune area ($h \geq 2 \text{ m}^* + \text{NAP}$)			Sandflat ($0.84 \text{ m}^{**} < h < 2 \text{ m}^* + \text{NAP}$)		
	deposition ($\Delta h \geq 0.1 \text{ m}$)	erosion ($\Delta h \leq -0.1 \text{ m}$)	net ($ \Delta h \geq 0.1 \text{ m}$)	deposition ($\Delta h \geq 0.1 \text{ m}$)	erosion ($\Delta h \leq -0.1 \text{ m}$)	net ($ \Delta h \geq 0.1 \text{ m}$)
1997-2006	1.12	-0.03	1.09	0.24	-0.03	0.21
2006-2011	0.74	-0.05	0.69	0.17	-0.05	0.12
2011-2015	0.72	-0.14	0.58	0.09	-0.06	0.03
1997-2015	2.55	-0.05	2.50	0.20	-0.03	0.17

* 2m criterion had to hold for last of the two surveys, separating the aeolian deposition area from the sandflat.

** 0.84m criterion had to hold for both surveys to consider only volume changes on the sandflat above MSHTL.

5. Discussion

In the previous section we described morphological changes that occurred both in the subtidal and subaerial part of the inlet system over the past decades. In the following we interpret these in term of possible sediment transport pathways connecting the two parts of the system. We start at the observation that the dune system gained about 2,5 million m^3 sand over the past 18 years (or on average about $0.14 \cdot 10^6 \text{ m}^3/\text{yr}$). Compared to the 9 million m^3 involved in shoreline erosion due to migration of the Molengat channel between 1986 and 2012 (or on average about $0.35 \cdot 10^6 \text{ m}^3/\text{yr}$), this appears to be a non-negligible amount. The question arises whether some of that nearshore sediment loss may have found its way to the rapidly expanding dune system on De Hors.

Starting from the 2.5 million m^3 volume increase of the dune system over the past 18 year, and an approximate surface area of De Hors sandflat above MSHTL of about 2 km^2 , this would translate to a lowering of the sandflat above MSHTL by approximately 1.3 m. This was not observed. To the contrary, the sandflat might even have gained a small amount of sediment volume. This implies that sediment losses from the sandflat due to aeolian transport must have been replenished by hydrodynamic processes or, alternatively, it might imply that the main source of sediment for aeolian transport was not the sandflat but the intertidal beach, as was suggested to be the case for a mega nourishment with a wide subaerial surface on the west coast of the Netherlands (Hoonhout and De Vries, 2017). In the latter case it was suggested that sorting processes acting on the surface sediments lead to armoring of the subaerial part of the sandflat reducing its capacity to act as a sediment source for aeolian transport. Either way, about $2.50 \cdot 10^6 \text{ m}^3$ was extracted from the subtidal system over the 18 year period.

The deposition observed to occur above MSHTL along the western margin of De Hors, is believed to occur during storm surge flooding as the more or less shore parallel erosion/deposition pattern bears resemblance to overwash deposition and berm formation rather than to net aeolian deposition, especially considering the predominantly southerly and southwesterly winds.

Another important observation is the consistently observed deposition of sediment near the southern tip of De Hors up to and even above MSHTL, providing a continuous fresh source of sediment for aeolian transport. It is proposed that the shoreline erosion at the west side of De Hors since 2006 is related to ongoing wave-driven erosion along the upper part of the cross-shore channel profile. Due to the wave sheltering effect of the ebb tidal delta, the net nearshore transport of sand along the SW- Texel coastline is directed to the south as waves from southerly directions dissipate on the Noorderhaaks sandflat. The deposition observed to occur on the southern tip of De Hors might thus be fed by this wave driven longshore transport.

Therefore, we propose two transport pathways for sediment from the subtidal to subaerial part of the inlet system. Firstly, through storm surge deposition on the sandflat above MSHTL and subsequent pick-up by wind during regular water levels; secondly, through intertidal deposition near the southern tip of De Hors and pick of sediment during lower tidal levels. To determine the role of storm surge deposition on the flat vs. the role of intertidal deposition on the south side of De Hors requires finer temporal resolution in the

topographic surveys to observe single storm surge deposition events and the disappearance of those deposits over time by aeolian transport over time. This would allow the assessment of the actual volume involved in this mechanism, hence we would know whether it can fully explain the dune volume increase, or whether the intertidal deposition areas play an important role too.

6. Conclusions

Based on the observed morphological changes, a conceptual model of sediment transport pathways for both the subtidal and subaerial components in the northern part of the inlet system is hypothesized, including the following components:

- In the shelter zone of the ebb-delta, the net nearshore transport of sand along the SW-Texel coastline is directed to the south as waves from southerly directions dissipate on the Noorderhaaks sandflat.
- The southward extension of De Hors sandflat is fed by this net nearshore transport.
- During storm surge flooding of De Hors sandflat, sediment is deposited onto the sandflat from the seaward side
- The increased area of freshly deposited sand on the south end of the beach plain, as well as storm deposits on the (under normal conditions) subaerial part of De Hors sandflat are then available for aeolian transport by the prevailing southerly winds, stimulating dune development on the northern end of the sandflat.

Future research will consider quantitative aspects of underlying transport processes to verify the proposed sediment transport pathways.

Acknowledgements

This research forms a component of the *CoCoChannel* project (Co-designing Coasts using natural Channel-shoal dynamics), which is funded by Netherlands Organization for Scientific Research, Earth Sciences division (NWO-ALW), and co-funded by Hoogheemraadschap Hollands Noorderkwartier. We further wish to acknowledge Rijkswaterstaat for making their valuable bathymetric and topographic data sets freely available, as well as the water level data.

References

- Aagaard, T., Davidson-Arnott, R., Greenwood, B., Nielsen, J., 2004. Sediment supply from shoreface to the dunes: linking sediment transport measurements and long-term morphological evolution. *Geomorphology*, 60: 205-224.
- Anthony, E.J., 2013. Storms, shoreface morphodynamics, sand supply, and the accretion and erosion of coastal dune barriers in the Southern North Sea. *Geomorphology*, 199: 8-21.
- Elias, E.P.L., Van der Spek, A.J.F., 2006. Long-term morphological evolution of Texel Inlet and its ebb-tidal delta (The Netherlands). *Marine Geology*, 225: 5-21.
- Hoonhout, B.M. and de Vries, S., 2017. Field measurements on spatial variations in aeolian sediment availability at the Sand Motor mega nourishment. *Aeolian Research*, 24: 93-104.
- Matias, A., Vila-Concejo, A., Ferreira, O., Morris, B., Alveirinho Dias, J., 2009. Sediment dynamics of barriers with frequent overwash. *J. Coastal Res.*, 25 (3): 768-780.
- Rosati, J.D. and G.W. Stone, 2009, Geomorphologic Evolution of Barrier Islands along the Northern U.S. Gulf of Mexico and Implications for Engineering Design in Barrier Restoration. *J. of Coastal Res.*, 25 (1): 8-22.
- Sallenger, A. H. J. (2000), Storm impact scale for barrier islands, *J. Coastal Res.*, 16: 890-895.